An Improved Transmission Matrix Formulation of Cascaded Discontinuities and its Application to *E*-Plane Circuits

RAAFAT R. MANSOUR, STUDENT MEMBER, IEEE, AND ROBERT H. MACPHIE, SENIOR MEMBER, IEEE

Abstract—**We study the effect of the relative convergence problem on the transmission matrix formulation of cascaded discontinuities. A numerically efficient modified formulation satisfying the edge condition is presented. Application is in the analysis of waveguiding structures in which a number of conductors are placed on various interfaces. Numerical results are presented for double-ridged waveguides and finlines. Applications to *E*-plane filters are also discussed.**

I. Introduction

THE MODAL ANALYSIS TECHNIQUE has been frequently used in solving waveguide junction scattering problems. The technique provides a formally exact solution with matrices of infinite size which must be truncated for numerical computation. It has been shown, however, in [1] that improper choice of the ratio between the number of modal terms retained in the guides forming the junction may lead to violation of the edge condition, which in turn leads to the relative convergence problem. On the other hand, convergence of the modal analysis solutions of some waveguide discontinuities has been studied in [2]–[4], where it is shown that as long as the number of modes used is large, the relative convergence problem does not affect the numerical solution significantly.

In this paper, we will show that the situation is different when we deal with discontinuities in cascade; the effect of the relative convergence on the numerical solution is noticeable and can be considered critical in some cases.

In a recent publication [5], it has been demonstrated that the transmission matrix representation of waveguide discontinuities is superior to the scattering matrix representation as far as the CPU time is concerned. It has, however, been stated that the transmission matrix formulation requires an equal number of modes to be retained in any of the guides forming the discontinuity. For some waveguide discontinuities, this requirement may violate the edge condition, resulting in incorrect numerical solutions.

We present a modified transmission matrix formulation with which the relative convergence problem can be avoided. This formulation is quite general and has a wide range of applications. To illustrate its applicability and to establish the accuracy of the numerical solution, which is the main emphasis in this paper, this formulation is employed with a transverse resonance concept to provide accurate and numerically efficient solutions for the propagation characteristics of double-ridged waveguides and finlines. We also show how this formulation can be adopted to provide an efficient analysis for metal-insert *E*-plane filters.

Manuscript received March 25, 1986; revised July 7, 1986. This work was supported in part by Grant A-2176 of the Natural Sciences and Engineering Research Council, Ottawa, Canada.

The authors are with the Department of Electrical Engineering, University of Waterloo, Waterloo, Ontario, Canada N2L 3G1.

IEEE Log Number 8610558.

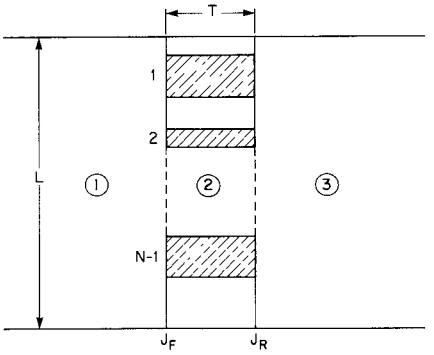

Fig. 1. An *N*-furcated cascaded waveguide discontinuity.

II. Cascaded Discontinuities and the Relative Convergence Problem

Consider the cascading of two *N*-furcated junctions, as shown in Fig. 1. Let junction $\mathbf{J}_F$ separate guides 1 and 2, whereas junction $\mathbf{J}_R$ separates guides 2 and 3. Let us also assume that P modes are retained in both guides 1 and 3, and Q modes in guide 2 (the *N*-furcated guide). This cascaded discontinuity can be treated by processing either the individual scattering matrices or the individual transmission matrices. The first approach does not require the use of an equal number of modes. The second one is faster; it does, however, require, as stated in [5], the same number of modes (i.e., P must be equal to Q).

If the scattering and transmission matrices of junctions $\mathbf{J}_F(\mathbf{J}_R)$ are, respectively, denoted by $\mathbf{S}^F(\mathbf{S}^R)$ and $\mathbf{T}^F(\mathbf{T}^R)$, the overall scattering and transmission matrices $\mathbf{S}^C, \mathbf{T}^C$ of the cascaded discontinuity can be written as

$$\mathbf{S}^C = \begin{bmatrix} \mathbf{S}_{11}^C & \mathbf{S}_{13}^C \\ \mathbf{S}_{31}^C & \mathbf{S}_{33}^C \end{bmatrix} \qquad \mathbf{T}^C = \begin{bmatrix} \mathbf{T}_{11}^C & \mathbf{T}_{13}^C \\ \mathbf{T}_{31}^C & \mathbf{T}_{33}^C \end{bmatrix}$$

0018-9480/86/1200-1490$01.00 ©1986 IEEE

where

$$\mathbf{S}_{11}^{C}=\mathbf{S}_{11}^{F}+\mathbf{S}_{12}^{F}\mathbf{L}^{-}\mathbf{S}_{22}^{R}\left(\mathbf{I}-\mathbf{L}^{-}\mathbf{S}_{22}^{F}\mathbf{L}^{-}\mathbf{S}_{22}^{R}\right)^{-1}\mathbf{L}^{-}\mathbf{S}_{21}^{F} \tag{1}$$

$$\mathbf{S}_{31}^{C}=\mathbf{S}_{32}^{R}\left(\mathbf{I}-\mathbf{L}^{-}\mathbf{S}_{22}^{F}\mathbf{L}^{-}\mathbf{S}_{22}^{R}\right)^{-1}\mathbf{L}^{-}\mathbf{S}_{21}^{F} \tag{2}$$

$$\mathbf{S}_{13}^{C}=\mathbf{S}_{12}^{F}\left(\mathbf{I}-\mathbf{L}^{-}\mathbf{S}_{22}^{R}\mathbf{L}^{-}\mathbf{S}_{22}^{F}\right)^{-1}\mathbf{L}^{-}\mathbf{S}_{23}^{R} \tag{3}$$

$$\mathbf{S}_{33}^{C}=\mathbf{S}_{33}^{R}+\mathbf{S}_{32}^{R}\mathbf{L}^{-}\mathbf{S}_{22}^{F}\left(\mathbf{I}-\mathbf{L}^{-}\mathbf{S}_{22}^{R}\mathbf{L}^{-}\mathbf{S}_{22}^{F}\right)^{-1}\mathbf{L}^{-}\mathbf{S}_{23}^{R} \tag{4}$$

$$\begin{bmatrix}\mathbf{T}_{11}^{C} & \mathbf{T}_{13}^{C}\\ \mathbf{T}_{31}^{C} & \mathbf{T}_{33}^{C}\end{bmatrix}=\begin{bmatrix}\mathbf{T}_{11}^{F} & \mathbf{T}_{12}^{F}\\ \mathbf{T}_{21}^{F} & \mathbf{T}_{22}^{F}\end{bmatrix}=\begin{bmatrix}\mathbf{L}^{+} & \mathbf{0}\\ \mathbf{0} & \mathbf{L}^{-}\end{bmatrix}\begin{bmatrix}\mathbf{T}_{22}^{R} & \mathbf{T}_{23}^{R}\\ \mathbf{T}_{32}^{R} & \mathbf{T}_{33}^{R}\end{bmatrix} \tag{5}$$

$$\mathbf{L}^{\pm}=\begin{bmatrix}\mathbf{L}_{1}^{\pm} & \mathbf{0} & — & — & \mathbf{0}\\ \mathbf{0} & \mathbf{L}_{2}^{\pm} & — & — & \mathbf{0}\\ — & — & — & — & —\\ — & — & — & — & —\\ \mathbf{0} & \mathbf{0} & — & — & \mathbf{L}_{N}^{\pm}\end{bmatrix}. \tag{6}$$

In (1)–(4), $\mathbf{I}$ is the identity matrix and $\mathbf{L}_{i}^{\pm}$, $i=1,2,\cdots,N$, are diagonal matrices whose diagonal elements are given by $L_{i,nn}^{\pm}=e^{\pm j\beta_{in}T}$, β_{in} being the propagation constant of the nth mode in the ith guide of the N-furcated section. Equations (1)–(5) are written in a general form; they can be further simplified as in the symmetric case of Fig. 1.

With $P=Q$, the numerical results reveal that both approaches fail to provide the correct solution as the septa thickness T gets smaller. This can be shown by plotting the magnitude of the tangential field at the junction. In Fig. 2, we choose a 4-furcated cascaded discontinuity as an example, and we plot the magnitude of E_x for different values of T/L with two ratios of mode numbers: $P/Q=1$ and $P/Q=R$, where R refers to the correct ratio [1]. It can be observed that for small values of T/L, using $P/Q=1$ violates not only the edge condition but also the boundary condition on the surface of the conducting septa.

We also consider the case of an inductive strip mounted in the E-plane of rectangular waveguide, which is the basic building block in the design of E-plane filters. The numerical results of the TE_{10} mode reflection and transmission coefficients are shown in Table I. It is noted that the effect of the ratio P/Q becomes considerable as T/L gets smaller, and with $P/Q=1$ the formulation completely collapses in the case of infinitely thin septa. This case has been mathematically investigated, and it is readily shown that *regardless of the matrix size* the formulation *always* collapses as long as $P/Q=1$.

In Fig. 3 we show the absolute convergence of the magnitude of the transmission coefficient $\mathbf{S}_{13}^{C}$ for $T/L=10^{-1}$ and $T/L=10^{-5}$ with different ratios of P/Q. Due to symmetry, a magnetic wall can be placed at the enter of the septa along the z-axis, and we only need to consider one-half of the structure. P and Q in this figure represent the number of modes retained in the large and small guides of the reduced structure, respectively. It is noted that the convergence rate is almost unaffected by the ratio

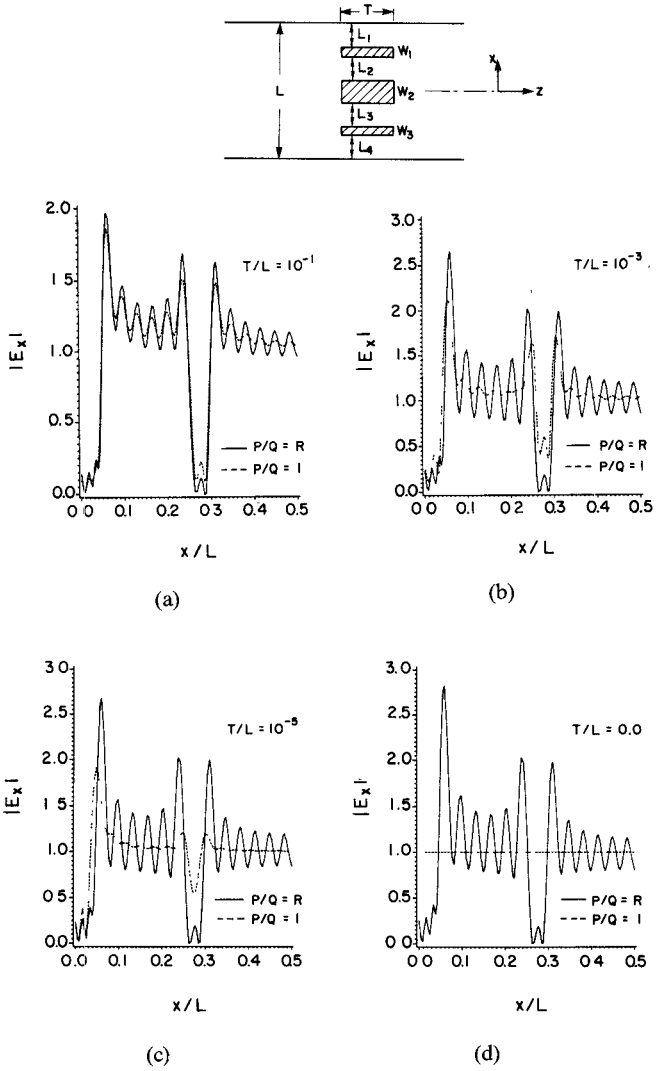

Fig. 2. Relative convergence problem demonstrated by field plots; $L_1=L_2=L_3=L_4=0.2L$, $W_1=W_3=0.05L$, $W_2=0.1L$, $R=L/(L_1+L_2+L_3+L_4)$, $Q=N_1+N_2+N_3+N_4$, $N_1/L_1=N_2/L_2=N_3/L_3=N_4/L_4$.

TABLE I
THE DOMINANT MODE REFLECTION AND TRANSMISSION COEFFICIENTS FOR DIFFERENT VALUES OF T/L

$\frac{T}{L}$	Reflection Coefficient		Transmission Coefficient	
	$\frac{P}{Q}=R$	$\frac{P}{Q}=1$	$\frac{P}{Q}=R$	$\frac{P}{Q}=1$
10^{-1}	-0.96671+j0.22400	-0.96653+j0.22460	0.02792+j0.12050	0.02807+j0.12079
10^{-3}	-0.92170+j0.26936	-0.91755+j0.27578	0.07829+j0.26791	0.08245+j0.27432
10^{-5}	-0.92012+j0.27112	-0.90437+j0.29410	0.07988+j0.27110	0.09564+j0.29408
0.0	-0.92011+j0.27114	0.00000+j0.00000	0.07989+j0.27114	1.00000+j0.00000

$L=7.112$ mm, $W=1.25$ mm, $f=26$ GHz, and $R=1.25$.

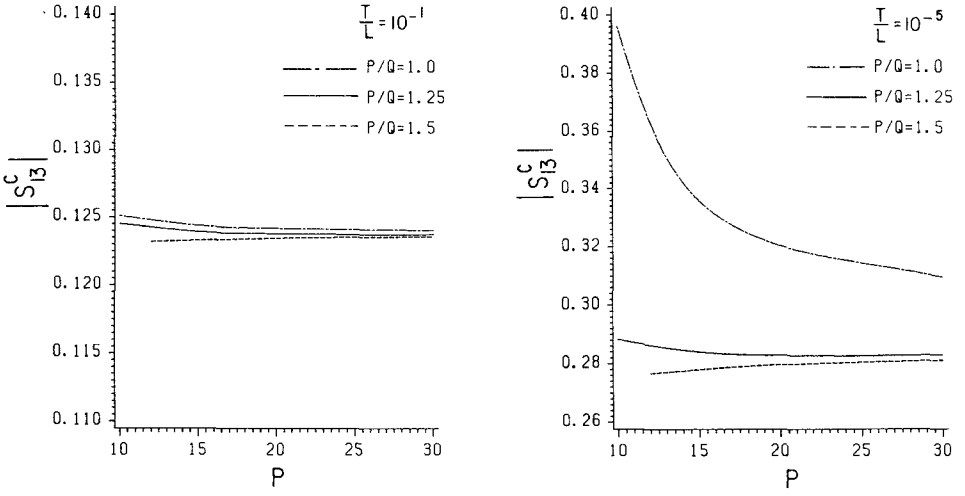

Fig. 3. Convergence of the magnitude of the transmission coefficient as a function of P with P/Q as parameters and for two cases $T/L=10^{-1}$, $T/L=10^{-5}$; dimensions according to Table I.

P/Q for $T/L=10^{-1}$, whereas in the case of $T/L=10^{-5}$ it is very slow when $P/Q=1$.

III. Matrix Representation of Waveguide Junctions

Refer to the junction $\mathbf{J}_F$ shown in Fig. 4. With P modes retained in guide 1 and Q modes in guide 2, applying the conservation of complex power technique CCPT [3] yields[1]

$$(\underline{A}_+ + \underline{A}_-) = \mathbf{H}_F(\underline{B}_+ + \underline{B}_-) \tag{7}$$

$$(\underline{A}_+ - \underline{A}_-)^\dagger \mathbf{P}_1(\underline{A}_+ + \underline{A}_-) = (\underline{B}_- - \underline{B}_+)^\dagger \mathbf{P}_2(\underline{B}_+ + \underline{B}_-) \tag{8}$$

where $\mathbf{H}_F$ is the E-field mode-matching matrix, and $\mathbf{P}_1$ and $\mathbf{P}_2$ are diagonal matrices whose diagonal elements are the powers carried by unit amplitude modes in guides 1 and 2, respectively. $\underline{A}$ and $\underline{B}$ are, respectively, the E-field mode amplitude vectors in guides 1 and 2. This junction can be represented either by the scattering matrix or by the transmission matrix. The parameters of the scattering and transmission matrices are related to the amplitude vectors $\underline{A}$ and $\underline{B}$ according to

$$\begin{bmatrix} \underline{A}_- \\ \underline{B}_- \end{bmatrix} = \begin{bmatrix} \mathbf{S}_{11}^F & \mathbf{S}_{12}^F \\ \mathbf{S}_{21}^F & \mathbf{S}_{22}^F \end{bmatrix} \begin{bmatrix} \underline{A}_+ \\ \underline{B}_+ \end{bmatrix} \tag{9}$$

$$\begin{bmatrix} \underline{A}_+ \\ \underline{A}_- \end{bmatrix} = \begin{bmatrix} \mathbf{T}_{11}^F & \mathbf{T}_{12}^F \\ \mathbf{T}_{21}^F & \mathbf{T}_{22}^F \end{bmatrix} \begin{bmatrix} \underline{B}_- \\ \underline{B}_+ \end{bmatrix}. \tag{10}$$

In view of [3], the scattering parameters can be written as

$$\mathbf{S}_{22}^F = \left(\mathbf{P}_2^\dagger + \mathbf{H}_F^\dagger \mathbf{P}_1^\dagger \mathbf{H}_F\right)^{-1}\left(\mathbf{P}_2^\dagger - \mathbf{H}_F^\dagger \mathbf{P}_1^\dagger \mathbf{H}_F\right) \tag{11}$$

$$\mathbf{S}_{12}^F = \mathbf{H}_F\left(\mathbf{I} + \mathbf{S}_{22}^F\right) \tag{12}$$

$$\mathbf{S}_{21}^F = 2\left(\mathbf{P}_2^\dagger + \mathbf{H}_F^\dagger \mathbf{P}_1^\dagger \mathbf{H}_F\right)^{-1} \mathbf{H}_F^\dagger \mathbf{P}_1^\dagger \tag{13}$$

$$\mathbf{S}_{11}^F = \mathbf{H}_F \mathbf{S}_{21}^F - \mathbf{I} \tag{14}$$

[1]The following notations are used: † denotes Hermitian transpose, all vectors are printed with underbar, and all matrices are printed in boldface.

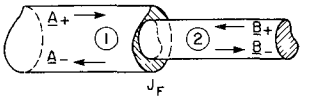

Fig. 4. Junction of two waveguides.

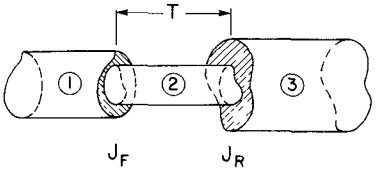

Fig. 5. A cascaded waveguide discontinuity.

where the dimensions of the matrices $\mathbf{H}_F$, $\mathbf{P}_1$, $\mathbf{P}_2$, $\mathbf{S}_{11}^F$, $\mathbf{S}_{12}^F$, $\mathbf{S}_{21}^F$, and $\mathbf{S}_{22}^F$ are, respectively, $(P\times Q)$, $(P\times P)$, $(Q\times Q)$, $(P\times P)$, $(P\times Q)$, $(Q\times P)$, and $(Q\times Q)$.

With $P=Q$, the parameters of the transmission matrix can be determined either by manipulating the basic CCPT equations (7), (8) in a similar fashion to what has been demonstrated in [3], or by simply substituting (11)–(14) into the following **S**-to-**T** transformation equations:

$$\mathbf{T}_{11} = [\mathbf{S}_{21}]^{-1} \tag{15}$$

$$\mathbf{T}_{21} = \mathbf{S}_{11}[\mathbf{S}_{21}]^{-1} \tag{16}$$

$$\mathbf{T}_{12} = -[\mathbf{S}_{21}]^{-1}\mathbf{S}_{22} \tag{17}$$

$$\mathbf{T}_{22} = -\mathbf{S}_{11}[\mathbf{S}_{21}]^{-1}\mathbf{S}_{22} + \mathbf{S}_{12}. \tag{18}$$

Following either methods yields

$$\mathbf{T}_{11}^F = \mathbf{T}_{22}^F = \frac{1}{2}\left[\mathbf{H}_F + \left[\mathbf{H}_F^\dagger \mathbf{P}_1^\dagger\right]^{-1}\mathbf{P}_2^\dagger\right] \tag{19}$$

$$\mathbf{T}_{12}^F = \mathbf{T}_{21}^F = \mathbf{T}_{11}^F - \left[\mathbf{H}_F^\dagger \mathbf{P}_1^\dagger\right]^{-1}\mathbf{P}_2^\dagger. \tag{20}$$

Equations (19) and (20) are similar in form to those derived in [5] using a different mode-matching method.

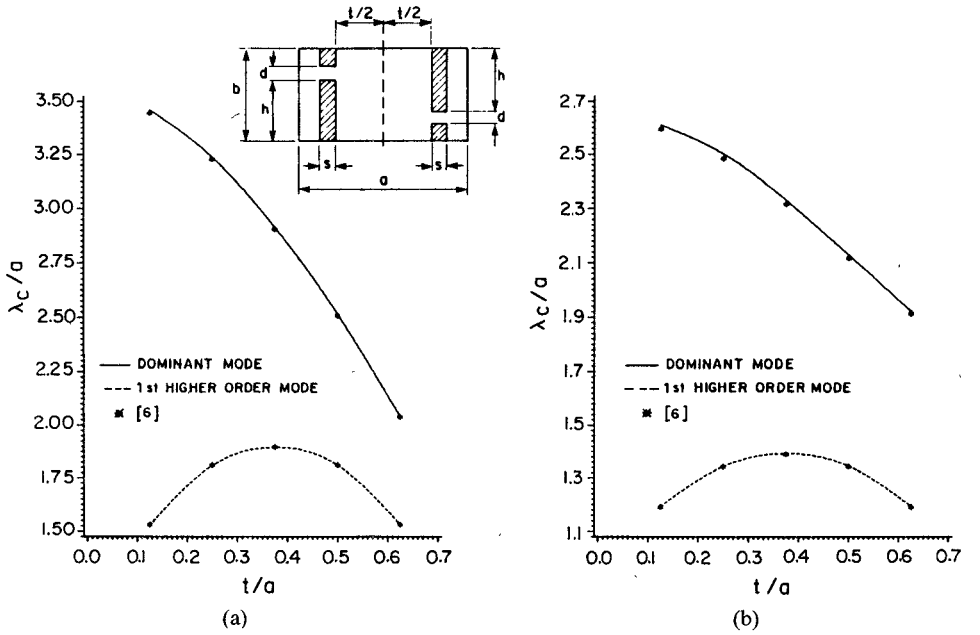

Fig. 6. Normalized cutoff wavelength λ_c/a of the dominant TE mode and the first higher order mode; $b/a = 0.5$, $s/a = 0.125$. (a) $d/b = 0.25$, $h/b = 0.375$. (b) $d/b = 0.5$, $h/b = 0.25$.

IV. Modified Formulation

Consider the cascaded waveguide discontinuity shown in Fig. 5. It is evident that the CPU time can be considerably reduced if this cascaded discontinuity is treated by the transmission matrix rather than the scattering matrix. However, the transmission matrix formulation which is derived in Section III assuming $P = Q$ has the following drawbacks.

1) As has been shown in Section II, using the same number of modes may lead to incorrect numerical solutions when the distance between the two junctions is relatively small.

2) There is unnecessarily large computational effort, especially when the distance T is relatively large. Although we may need a large number of modes to correctly describe junctions $\mathbf{J}_F$ and $\mathbf{J}_R$, only a few modes are usually required in this case to correctly include the coupling between the two junctions. Thus, using more modes in guide 2 does not significantly contribute to the numerical solution but increases the CPU time required to evaluate the overall transmission matrix.

The idea of the modified formulation stems from the observation about the generalized scattering matrix analysis described by (1)–(4): that the parameters of the first Q modes of $\mathbf{S}^C$ will be *unchanged* if $\mathbf{S}_{11}^F$, $\mathbf{S}_{12}^F$, $\mathbf{S}_{21}^F$, $\mathbf{S}_{22}^F$, $\mathbf{S}_{22}^R$, $\mathbf{S}_{23}^R$, $\mathbf{S}_{32}^R$, and $\mathbf{S}_{33}^R$ on the right-hand side of (1)–(4) are replaced, respectively, by $\mathbf{S}_{11Q}^F$, $\mathbf{S}_{12Q}^F$, $\mathbf{S}_{21Q}^F$, $\mathbf{S}_{22Q}^F$, $\mathbf{S}_{22Q}^R$, $\mathbf{S}_{23Q}^R$, $\mathbf{S}_{32Q}^R$, and $\mathbf{S}_{33Q}^R$. The matrices in the latter set are square matrices of order $(Q \times Q)$ obtained by partitioning the corresponding matrices in the former set.

In view of this observation, the modified elements of the transmission matrix are obtained by first partitioning the matrices given in (11)–(14) to get another set of square matrices $\mathbf{S}_{11Q}^F$, $\mathbf{S}_{12Q}^F$, $\mathbf{S}_{21Q}^F$, and $\mathbf{S}_{22Q}^F$ of order $(Q \times Q)$; these partitioned matrices are then substituted into (15)–(18). After some manipulations, we get

$$\mathbf{T}_{11}^F = \frac{1}{2}\left[\mathbf{P}_{1Q}^\dagger\right]^{-1}\left[\mathbf{H}_{FQ}^\dagger\right]^{-1}\left[\mathbf{H}_F^\dagger \mathbf{P}_1^\dagger \mathbf{H}_F + \mathbf{P}_2^\dagger\right] \tag{21}$$

$$\mathbf{T}_{12}^F = \mathbf{T}_{11}^F - \left[\mathbf{P}_{1Q}^\dagger\right]^{-1}\left[\mathbf{H}_{FQ}^\dagger\right]^{-1}\mathbf{P}_2^\dagger \tag{22}$$

$$\mathbf{T}_{21}^F = \mathbf{H}_{FQ} - \mathbf{T}_{11}^F \tag{23}$$

$$\mathbf{T}_{22}^F = \mathbf{H}_{FQ} - \mathbf{T}_{12}^F. \tag{24}$$

By renaming the subscripts of the scattering parameters in (11)–(14) and following the same procedures, the parameters of $\mathbf{T}^R$ can be written as

$$\mathbf{T}_{22}^R = \frac{1}{2}\left[\mathbf{P}_2^\dagger\right]^{-1}\left[\mathbf{P}_2^\dagger + \mathbf{H}_R^\dagger \mathbf{P}_3^\dagger \mathbf{H}_R\right]\left[\mathbf{H}_{RQ}\right]^{-1} \tag{25}$$

$$\mathbf{T}_{23}^R = \mathbf{T}_{22}^R - \left[\mathbf{P}_2^\dagger\right]^{-1}\mathbf{H}_{RQ}^\dagger \mathbf{P}_{3Q}^\dagger \tag{26}$$

$$\mathbf{T}_{32}^R = \left[\mathbf{H}_{RQ}\right]^{-1} - \mathbf{T}_{22}^R \tag{27}$$

$$\mathbf{T}_{33}^R = \left[\mathbf{H}_{RQ}\right]^{-1} - \mathbf{T}_{23}^R. \tag{28}$$

$\mathbf{H}_{FQ}$, $\mathbf{H}_{RQ}$, $\mathbf{P}_{1Q}$, and $\mathbf{P}_{3Q}$ are square matrices of order $(Q \times Q)$ and are obtained by partitioning, respectively, the matrices $\mathbf{H}_F$, $\mathbf{H}_R$, $\mathbf{P}_1$, and $\mathbf{P}_3$. The overall transmission matrix $\mathbf{T}^C$ can then be evaluated by using simple matrix multiplications according to (5). It is interesting to note that in the case of symmetry $\mathbf{H}_R = \mathbf{H}_F$, $\mathbf{P}_3 = \mathbf{P}_1$ and we only need to invert *one frequency-independent matrix* $\mathbf{H}_{FQ}$ since matrices $\mathbf{P}_{1Q}$ and $\mathbf{P}_2$ are diagonal matrices.

Applying the scattering matrix analysis with P, Q, and K modes in guides 1, 2, and 3, respectively, yields an overall scattering matrix $\mathbf{S}^C$ with matrices of $\mathbf{S}_{11}^C$, $\mathbf{S}_{13}^C$, $\mathbf{S}_{31}^C$, and $\mathbf{S}_{33}^C$ whose dimensions are, respectively, $(P \times P)$, $(P \times K)$, $(K \times P)$, and $(K \times K)$. If these matrices are partitioned to get another set of square matrices $\mathbf{S}_{11Q}^C$, $\mathbf{S}_{13Q}^C$, $\mathbf{S}_{31Q}^C$, and $\mathbf{S}_{33Q}^C$, the resulting scattering matrix relates Q

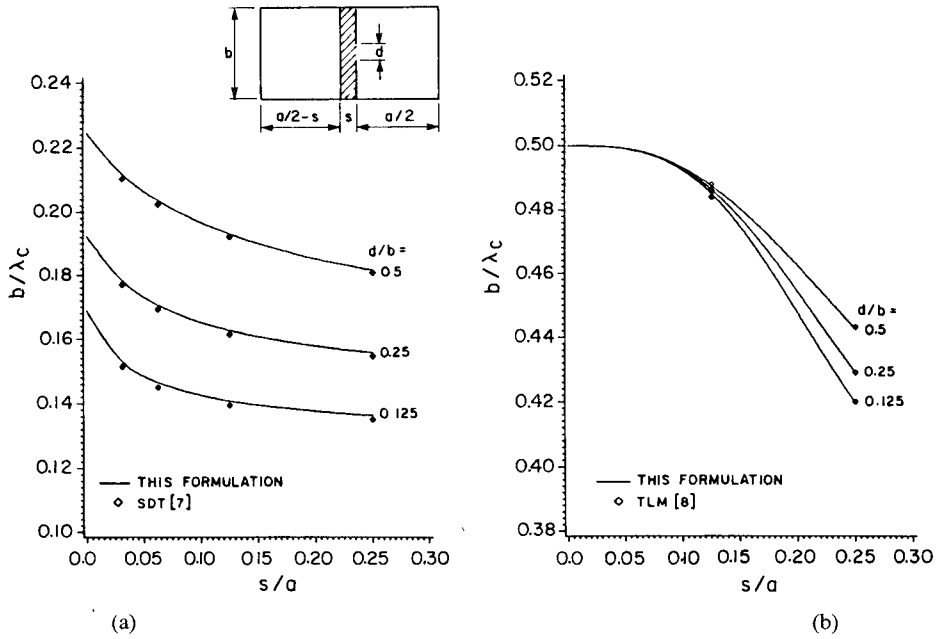

Fig. 7. Normalized cutoff frequencies b/λ_c in unilateral finlines; $b/a = 0.5$, $\varepsilon_r = 2.2$. (a) Dominant mode. (b) Second-order mode.

modes in guide 1 to Q modes in guide 3. It is important to note that there is a one-to-one correspondence between the two sets $(\mathbf{S}^C_{11Q}, \mathbf{S}^C_{13Q}, \mathbf{S}^C_{31Q}, \mathbf{S}^C_{33Q})$, $(\mathbf{T}^C_{11}, \mathbf{T}^C_{13}, \mathbf{T}^C_{31}, \mathbf{T}^C_{33})$; i.e., one set can be obtained from the other by S-to-T or T-to-S transformation. It should also be mentioned that limiting the overall scattering matrix or the overall transmission matrix to only Q modes where $Q < P, K$ does not mean that we lose any important information since P, Q, and K can be chosen as large as we need.

In order to check the numerical accuracy of this formulation, we consider the double-ridged waveguide shown in Fig. 6. In view of the proposed formulation and by simple matrix multiplications, the overall transmission matrix defined at the conducting terminal planes can be easily determined. Applying then the transverse resonance technique yields the eigenvalue equation which can be solved for the cutoff frequencies. Fig. 6 shows λ_c/a for the TE dominant and the first higher order mode. It is noted that our results are in good agreement with those given in [6].

In Fig. 7, we compare our results for the cutoff frequencies of unilateral finlines with those obtained using the spectral-domain technique [7] and the TLM method [8]. Results agree within 1 percent when the size of the eigenvalue matrix is chosen to be (4×4). It is interesting to note that in this example the fins are assumed to have a zero metallization thickness; this further emphasizes that our formulation can be applied even in the case of infinitely thin septa.

Although in this contribution we consider only two examples to demonstrate how fast and accurate numerical solutions can be provided by the proposed formulation, its simplicity in computing the dispersion characteristics of more complex waveguiding structures will be shown elsewhere [9].

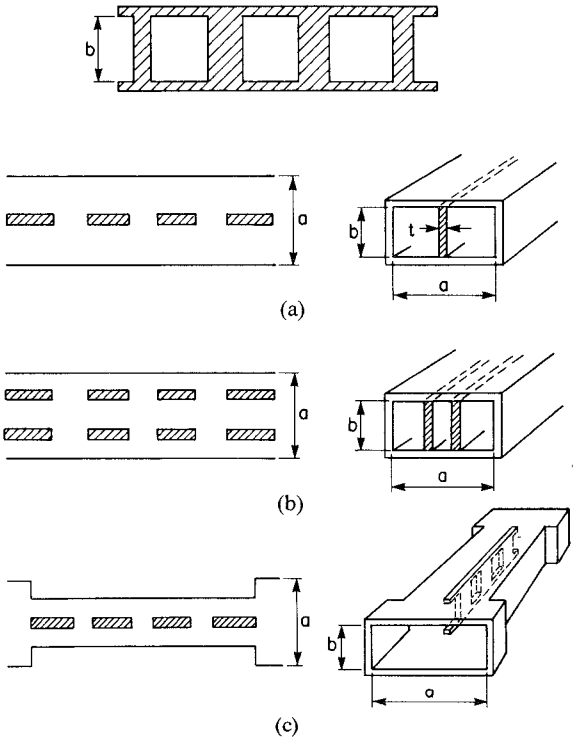

Fig. 8. Three configurations of metal-insert E-plane filters.

V. Application to Metal-Insert E-Plane Filters

E-plane filters in the form of metal inserts mounted in the E-plane of a rectangular waveguide have been widely used as low-cost, mass-producible circuits in millimeter-wave applications. Fig. 8 shows three configurations of metal-insert E-plane filters. These three filter configura-

tions have been separately analyzed in the literature [10]–[14]; in most cases the analysis starts with a modal matching method to determine the scattering matrix of the waveguide junction formed by the semi-infinite septa; then the generalized scattering matrix analysis is used repeatedly to find the overall scattering matrix of the filter.

In view of the N-furcated cascaded waveguide discontinuity shown in Fig. 1, one could consider the filter configurations shown in Fig. 8(a)–(c) as, respectively, 2-furcated, 3-furcated, and 4-furcated junctions connected in cascade. Because there is no structural variation in the y direction, only TE_{n0} modes will be excited in the case of TE_{10} incident mode. Thus, (11)–(14), which have been derived by the authors in [3] for scattering at an N-furcated junction, can be used with (1)–(4) to provide a unified treatment for metal-insert E-plane filters.

In the design of E-plane filters, a CAD algorithm based on an accurate analysis is used to tune the filter for a prescribed frequency response. Because of the CPU time required in the optimization process, the cost of generating acceptable design parameters is often prohibitively large. A considerable reduction in CPU time can be achieved if the filter sections are cascaded within the scheme of the transmission matrices rather than the scattering matrices. However, this method cannot be applied directly because of the problem of the numerical instability which may arise when many matrix multiplications are performed on matrices containing very large numbers. This problem has been discussed in [5] and an approach has been suggested to circumvent it.

We present here a more efficient approach to alleviate this problem. The advantage of this approach over that suggested in [5] is that it completely avoids using the generalized scattering matrix analysis where the larger computational effort is involved.

Let the parameters of the transmission matrix be written as

$$\underline{A}_{2+} = \mathbf{T}_{11}\underline{A}_{1+} + \mathbf{T}_{12}\underline{A}_{1-} \tag{29}$$

$$\underline{A}_{2-} = \mathbf{T}_{21}\underline{A}_{1+} + \mathbf{T}_{22}\underline{A}_{1-}. \tag{30}$$

If $\underline{A}_{1+}$ and $\underline{A}_{1-}$ are related according to

$$\underline{A}_{1-} = [\mathbf{L}^{-}\mathbf{S}^{(1)}\mathbf{L}^{-}]\underline{A}_{1+} \tag{31}$$

it can be shown that

$$\underline{A}_{2-} = \mathbf{S}^{(2)}\underline{A}_{2+}$$

$$\mathbf{S}^{(2)} = [\mathbf{T}_{21} + \mathbf{T}_{22}[\mathbf{L}^{-}\mathbf{S}^{(1)}\mathbf{L}^{-}]][\mathbf{T}_{11} + \mathbf{T}_{12}[\mathbf{L}^{-}\mathbf{S}^{(1)}\mathbf{L}^{-}]]^{-1}. \tag{32}$$

In the case of longitudinally symmetric structures such as E-plane filters, we only need to analyze half of the structure with electric and magnetic wall terminations. Thus, we first collect the discontinuities in the reduced structure (half the original one) into groups $1,2,\cdots,k$ separated by uniform line sections, as shown in Fig. 9. Within each group the discontinuities are cascaded by simple matrix multiplications of transmission matrices. We next terminate the reduced structure by magnetic and electric walls, which can be achieved by setting $\mathbf{S}_m^{(1)} = \mathbf{I}$

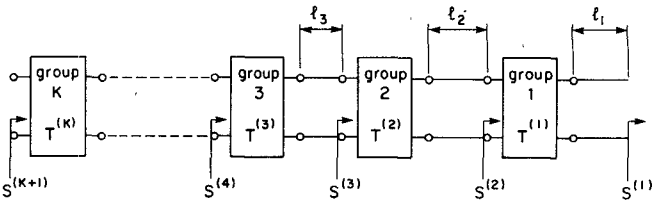

Fig. 9. Collecting cascaded discontinuities into groups separated by uniform line sections.

and $\mathbf{S}_e^{(1)} = -\mathbf{I}$. Substituting in (32) gives $\mathbf{S}_m^{(2)}$ and $\mathbf{S}_e^{(2)}$. $[\mathbf{L}_2^{-}\mathbf{S}_m^{(2)}\mathbf{L}_2^{-}]$ and $[\mathbf{L}_2^{-}\mathbf{S}_e^{(2)}\mathbf{L}_2^{-}]$ represent then the terminations seen at the output port of group 2 when the reduced structure is terminated, respectively, by magnetic and electric walls. The matrices $\mathbf{L}_i^{-}, i = 1,2,\cdots,k$, are diagonal matrices with diagonal elements $L_{in} = e^{-j\beta_n l_i}$, where l_i for $i = 1,2,\cdots,k$ are the lengths of the uniform line sections separating the groups shown in Fig. 9. Back substitution of $\mathbf{S}_m^{(2)}$ and $\mathbf{S}_e^{(2)}$ into (32) gives $\mathbf{S}_m^{(3)}$ and $\mathbf{S}_e^{(3)}$, and the procedure is repeated until we get $\mathbf{S}_m^{(k+1)}$ and $\mathbf{S}_e^{(k+1)}$. This can be mathematically expressed as

$$\mathbf{S}_m^{(1)} = \mathbf{I}$$

$$\mathbf{S}_e^{(1)} = -\mathbf{I}$$

$$\mathbf{S}_m^{(2)} = \left[\mathbf{T}_{21}^{(1)} + \mathbf{T}_{22}^{(1)}\left[\mathbf{L}_1^{-}\mathbf{S}_m^{(1)}\mathbf{L}_1^{-}\right]\right] \cdot \left[\mathbf{T}_{11}^{(1)} + \mathbf{T}_{12}^{(1)}\left[\mathbf{L}_1^{-}\mathbf{S}_m^{(1)}\mathbf{L}_1^{-}\right]\right]^{-1}$$

$$\mathbf{S}_e^{(2)} = \left[\mathbf{T}_{21}^{(1)} + \mathbf{T}_{22}^{(1)}\left[\mathbf{L}_1^{-}\mathbf{S}_e^{(1)}\mathbf{L}_1^{-}\right]\right] \cdot \left[\mathbf{T}_{11}^{(1)} + \mathbf{T}_{12}^{(1)}\left[\mathbf{L}_1^{-}\mathbf{S}_e^{(1)}\mathbf{L}_1^{-}\right]\right]^{-1}$$

$$\mathbf{S}_m^{(3)} = \left[\mathbf{T}_{21}^{(2)} + \mathbf{T}_{22}^{(2)}\left[\mathbf{L}_2^{-}\mathbf{S}_m^{(2)}\mathbf{L}_2^{-}\right]\right] \cdot \left[\mathbf{T}_{11}^{(2)} + \mathbf{T}_{12}^{(2)}\left[\mathbf{L}_2^{-}\mathbf{S}_m^{(2)}\mathbf{L}_2^{-}\right]\right]^{-1}$$

$$\mathbf{S}_e^{(3)} = \left[\mathbf{T}_{21}^{(2)} + \mathbf{T}_{22}^{(2)}\left[\mathbf{L}_2^{-}\mathbf{S}_e^{(2)}\mathbf{L}_2^{-}\right]\right] \cdot \left[\mathbf{T}_{11}^{(2)} + \mathbf{T}_{12}^{(2)}\left[\mathbf{L}_2^{-}\mathbf{S}_e^{(2)}\mathbf{L}_2^{-}\right]\right]^{-1}$$

$$\vdots$$

$$\mathbf{S}_m^{(k+1)} = \left[\mathbf{T}_{21}^{(k)} + \mathbf{T}_{22}^{(k)}\left[\mathbf{L}_k^{-}\mathbf{S}_m^{(k)}\mathbf{L}_k^{-}\right]\right] \cdot \left[\mathbf{T}_{11}^{(k)} + \mathbf{T}_{12}^{(k)}\left[\mathbf{L}_k^{-}\mathbf{S}_m^{(k)}\mathbf{L}_k^{-}\right]\right]^{-1}$$

$$\mathbf{S}_e^{(k+1)} = \left[\mathbf{T}_{21}^{(k)} + \mathbf{T}_{22}^{(k)}\left[\mathbf{L}_k^{-}\mathbf{S}_e^{(k)}\mathbf{L}_k^{-}\right]\right] \cdot \left[\mathbf{T}_{11}^{(k)} + \mathbf{T}_{12}^{(k)}\left[\mathbf{L}_k^{-}\mathbf{S}_e^{(k)}\mathbf{L}_k^{-}\right]\right]^{-1}.$$

The overall scattering parameters of the filter, $\mathbf{S}_{11}$, $\mathbf{S}_{12}$, $\mathbf{S}_{21}$, and $\mathbf{S}_{22}$ are then given by

$$\mathbf{S}_{11} = \mathbf{S}_{22} = \frac{1}{2}\left[\mathbf{S}_m^{(k+1)} + \mathbf{S}_e^{(k+1)}\right] \tag{33}$$

$$\mathbf{S}_{12} = \mathbf{S}_{21} = \frac{1}{2}\left[\mathbf{S}_m^{(k+1)} - \mathbf{S}_e^{(k+1)}\right]. \tag{34}$$

If the discontinuities in the filter are collected into groups, as shown in Fig. 10, the transmission matrix of each group can be calculated without any numerical prob-

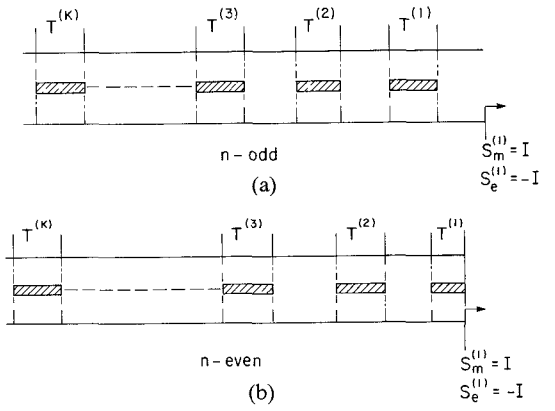

Fig. 10. Collecting cascaded discontinuities in the reduced structure (half the original filter structure) into groups.

TABLE II
THE NUMBER OF FREQUENCY-DEPENDENT MATRIX INVERSIONS REQUIRED BY THE PROPOSED APPROACH AND BY THE CONVENTIONAL APPROACH

Number of Resonators	The Proposed Approach	The Conventional Approach
n (odd) 3,5,7.....	$(n+1)$	$\frac{3}{2}(n+1)$
n (even) 2,4,6.....	$(n+2)$	$(\frac{3}{2}n+2)$

TABLE III
THE DIMENSIONS OF THE FILTERS SHOWN IN FIGS. 11, 12, 13, AND 14

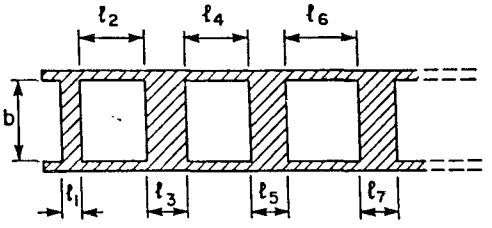

Waveguide dimensions	Number of resonators	Insert thickness	l_1 l_N	l_2 l_{N-1}	l_3 l_{N-2}	l_4 l_{N-3}	l_5 l_{N-4}	l_6 l_{N-5}	l_7 l_{N-6}	l_8 l_{N-7}	Figure
Ka-band a=7.112 b=3.556	3	1.250	0.7721	3.9527	3.4254	3.9593					Fig.(11)
W-band a=2.54 b=1.27	4	0.050	0.5990	1.4390	1.8110	1.4400	2.0080				Fig (12)
Ka-band a=7.112 b=3.556	7	0.025	0.1081	4.8556	0.6668	5.0978	0.9718	5.1369	1.0510	5.1427	Fig.(13)
Ka-band a=7.112 b=3.556	7	0.025	0.1541	3.2116	0.7753	3.2314	1.1652	3.2196	1.2802	3.2171	Fig.(14)

$N = 2n + 1$, where n is the number of resonators. All dimensions are in millimeters.

lems. Table II shows the number of frequency-dependent matrix inversions required in computing the overall scattering matrix of the filter by this approach and by the conventional approach used in [10]–[14], where the discontinuities are cascaded within the scheme of scattering matrices. It is noted that the computation effort is considerably reduced by applying the proposed approach; for example, in the case of a filter of $n = 7$, where n is the number of resonators, the conventional approach requires 12 frequency-dependent matrix inversions whereas the proposed approach requires only eight frequency-dependent matrix inversions in addition to the one matrix inversion required in inverting the frequency-independent matrix $\mathbf{H}_{FQ}$. Moreover, in view of the number of matrix multiplications involved in (1)–(4), it can be readily concluded that the proposed approach also requires a smaller number of matrix multiplications. This comparison indicates the efficiency of our approach, especially when it is used in the computer-aided design of E-plane filters, where the filter analysis has to be repeated many times at different frequencies.

To verify the reliability of this method, we consider filters of three, four, and seven resonators with dimensions as shown in Table III, and we compare our calculated results with those obtained using the conventional approach [10]–[14]. The comparison is given in Figs. 11–13, where it is noted that there is good agreement in all cases. The results shown in these figures are calculated based on the scheme described in Fig. 10 using 12 modes to include the higher order mode coupling between the inductive septa.

For filters of wide bandwidths, the lengths of the inductive septa are relatively short and one can achieve further reduction in computation time without having any numeri-

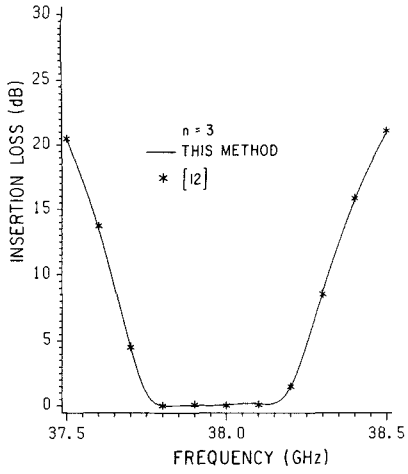

Fig. 11. Comparison of insertion loss results calculated by this method and by the conventional approach (graphical reproduction from [12]); data according to Table III; discontinuities are collected into two groups.

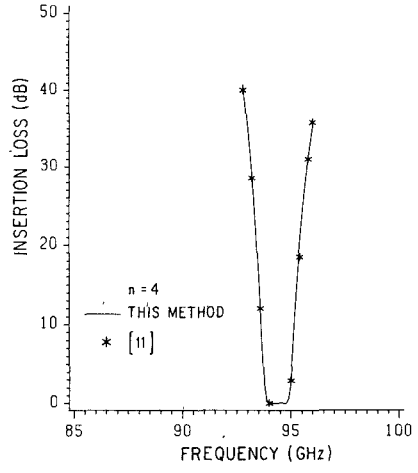

Fig. 12. Comparison of insertion loss results calculated by this method and by the conventional approach (graphical reproduction from [11]); data according to Table III; discontinuities are collected into three groups.

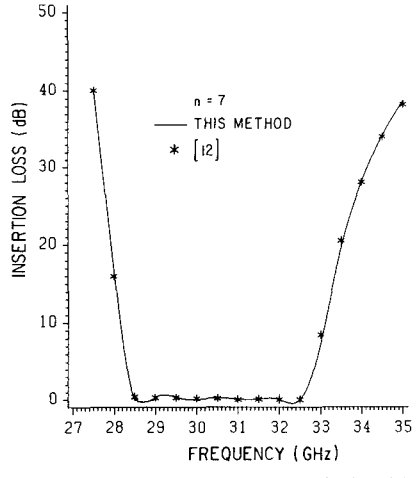

Fig. 13. Comparison of insertion loss results calculated by this method and by the conventional approach (graphical reproduction from [12]); data according to Table III; discontinuities are collected into four groups.

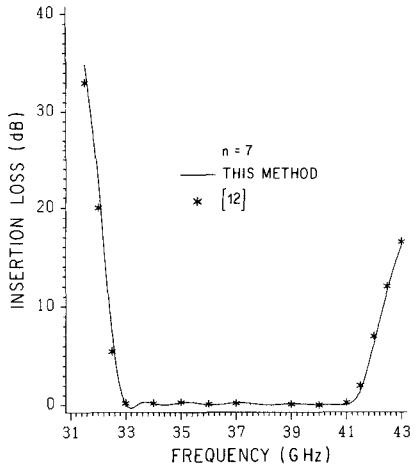

Fig. 14. Comparison of insertion loss results calculated by this method and by the conventional approach (graphical reproduction from [12]); data according to Table III; discontinuities are collected into two groups.

cal problems by combining two successive groups into one group. For example, in Fig. 14 we show the results calculated for a filter of $n = 7$ with a relatively wide bandwidth by collecting the cascaded discontinuities into two groups rather than four groups. Evaluation of the overall scattering matrix of the filter in this case requires only four frequency-dependent matrix inversions in addition to the frequency-independent matrix inversion required to invert $\mathbf{H}_{FQ}$.

Another possible application of this approach is in the design of optimized multisection transformers. In this case, we terminate the structure by a matched load, i.e., we set $\mathbf{S}^{(1)} = \mathbf{0}$ where $\mathbf{0}$ is the null matrix; the reflection coefficient at the transformer input can then be obtained by repeatedly using (32) until we get $\mathbf{S}^{(k+1)}$.

VI. Conclusions

It has been shown that even with the use of large numbers of modes, the relative convergence problem may seriously affect the modal analysis solution when we deal with discontinuities in cascade. The efficiency of the modified transmission matrix formulation presented here has been confirmed by comparing our numerical results for double-ridged waveguides and finlines with other published results. Moreover, a simple and unified approach has been introduced to analyze metal-insert E-plane filters. This is an improvement over the conventional approach used in the literature in that it provides accurate results with a considerable reduction in computation time.

References

[1] R. Mittra and S. W. Lee, *Analytic Techniques in the Theory of Guided Waves*. New York: Macmillan, 1971.

[2] Y. C. Shih and K. G. Gray, "Convergence of numerical solutions of step-type waveguide discontinuity problems by modal analysis," in *1983 IEEE MTT-S Dig.*, pp 233–235.

[3] R. R. Mansour and R. H. MacPhie, "Scattering at an N-furcated parallel plate waveguide junction," *IEEE Trans. Microwave Theory Tech.*, vol. MTT-33, pp. 830–835, Sept. 1985.

[4] T. S. Chu, T. Itoh, and Y. C. Shih, "Comparative study of mode matching formulations for microstrip discontinuity problems," *IEEE Trans. Microwave Theory Tech.*, vol. MTT-33, pp. 1018–1023, Oct. 1985.
[5] A. S. Omar and K. Schunemann, "Transmission matrix representation of finline discontinuities," *IEEE Trans. Microwave Theory Tech.*, vol. MTT-33, pp. 765–770, Sept. 1985.
[6] D. Dasgupta and P. K. Saha, "Eigenvalue spectrum of rectangular waveguide with two symmetrically placed double ridges," *IEEE Trans. Microwave Theory Tech.*, vol. MTT-29, pp. 47–51, Jan. 1981.
[7] A. K. Sharma and W. J. R. Hoefer, "Empirical expressions for fin-line design," *IEEE Trans. Microwave Theory Tech.*, vol. MTT-31, pp. 350–355, Apr. 1983.
[8] Y. C. Shih and W. J. R. Hoefer, "Dominant and second-order mode cutoff frequencies in fin lines calculated with a two-dimensional TLM program," *IEEE Trans. Microwave Theory Tech.*, vol. MTT-28, pp. 1443–1448, Dec. 1980.
[9] R. R. Mansour and R. H. MacPhie, "A unified hybrid-mode analysis for planar transmission lines," to be published.
[10] Y. C. Shih and T. Itoh, "*E*-plane filters with finite thickness septa," *IEEE Trans. Microwave Theory Tech.*, vol. MTT-31, pp. 1009–1012, Dec. 1983.
[11] R. Vahlhieck *et al.*, "*W*-band low insertion-loss *E*-plane filter," *IEEE Trans. Microwave Theory Tech.*, vol. MTT-32, pp. 133–135, Jan. 1984.
[12] Y. C. Shih, "Design of waveguide *E*-plane filters with all metal insert," *IEEE Trans. Microwave Theory Tech.*, vol. MTT-32, pp. 695–704, July 1984.
[13] F. Arndt *et al.*, "*E*-plane integrated filters with improved stopband attenuation," *IEEE Trans. Microwave Theory Tech.*, vol. MTT-32, pp. 1391–1394, Oct. 1984.
[14] R. Vahldieck and W. R. J. Hoefer, "Finline and metal insert filters with improved passband separation and increased stopband attenuation," *IEEE Trans. Microwave Theory Tech.*, vol. MTT-33, pp. 1333–1339, Dec. 1985.

Raafat R. Mansour (S'84) was born in Cairo, Egypt, on March 31, 1955. He received the B.Sc (with honors) and M.Sc degrees in electrical engineering from Ain Shams University, Cairo, in 1977 and 1981, respectively. Currently, he is working towards the Ph.D. degree at the University of Waterloo, Ontario, Canada.

He was a research fellow at the Laboratoire d'Electromagnétisme, Institut National Polytechnique, Grenoble, France, in 1981. Since 1983, he has been a Research and Teaching Assistant with the Department of Electrical Engineering, University of Waterloo. His present research interests are in the analysis and design of microwave and millimeter-wave integrated circuits.

✠

Robert H. MacPhie (S'57-M'63-SM'79) was born in Weston, Ontario, Canada, on September 20, 1934. He received the B.A.Sc. degree in electrical engineering from the University of Toronto in 1957 and the M.S. and Ph.D. degrees from the University of Illinois, Urbana, in 1959 and 1963, respectively.

In 1963, he joined the University of Waterloo, Waterloo, Ontario, Canada, as an Assistant Professor in Electrical Engineering and at present he is Professor of Electrical Engineering at Waterloo. His research interests currently focus on dipole antennas, waveguide scattering theory, scattering from prolate spheroid systems, and microstrip structures. During 1984–1985, he was on sabbatical leave as a Professeur Associé at the Université of Aix-Marseille I, France, working at the Département de Radioélectricité.